RSC Advances

RSC Advances

COMMUNICATION

Low temperature synthesis of carbon fibres and metal-filling carbon nanoparticles with laser irradiation into near-critical benzene

Takahiro Fukuda,[a] Yasuhiro Hayasaki,[b] Takashi Hasumura,[a] Yoshihiro Katsube,[b] Raymond L.D. Whitby[cd] and Toru Maekawa*[ab]

We irradiate near-critical benzene set at 290 °C, in which either an alloy rod composed of mainly iron, chromium, and nickel is placed or copper complex molecules; bis(t-butylacetoacetato)copper(II): $Cu(tbaoac)_2$, are dissolved, with the second (532 nm wavelength), third (355 nm), and fourth (266 nm) harmonics generated from a neodymium doped yttrium/aluminium/garnet (Nd:YAG) laser and show that carbon structures such as fibres, coils, and metal-filling carbon nanoparticles are efficiently produced. The operational temperature is 290 °C, which is much lower than that in the conventional synthetic methods of nano materials, and the laser power density can be as low as 3.9 mW mm^{-2}.

A variety of structures are formed by carbon; e.g., diamond, fibres, fullerenes, nanotubes, and graphene.[1-5] Several carbon nano/micro materials have already been used in various fields including mechanical, aeronautical, electronic, and biological engineering and technology thanks to their unique mechanical, electronic, and chemical properties. Carbon fibres, in particular, are known as an important industrial material and have been actively used in aircrafts, vehicles, and sports gear due to their lightness, flexibility, and strength, whereas carbon coils; one type of carbon fibres, are expected to be utilised as electromagnetic absorbers, micro-aerials, and intelligent tactile sensors.[6] Metal-filling carbon nanostructures are also of great importance particularly in the field of bio-medicine; e.g., metal-filling carbon nanostructures may well be used as bio-imaging agents, nano media for hyperthermia, and nano vehicles for drug delivery.[7-9] Carbon materials such as fullerenes, carbon nanotubes (CNTs), graphene, fibres, and coils are commonly produced by arc discharge,[4] laser ablation,[10,11] and chemical vapour deposition (CVD).[12]

It is well known that the gas-liquid coexistence curves terminate at the critical points, where clusters formed by the fluids' molecules percolate the fluids' systems.[13] As a result, incident light, scattered by the clusters, cannot penetrate the fluids' systems when the fluids' conditions are set at or near their critical points; known as *critical opalescence*.[13] Near- and super-critical fluids are extremely interesting and important from a fundamental scientific point of view thanks to their unique physical properties, universal features in the static and dynamic structures, and nonequilibrium transport characteristics.[13-18] Super-critical fluids are also important from technical and engineering points of view. They are often used in chemical, electronic, and environmental sciences and engineering; e.g., reactions are encouraged,[19,20] chemicals are extracted,[21,22] and semiconductors are cleaned and purified.[23,24] Nanomaterials can also be efficiently synthesised using super-critical fluids; e.g., nano/micro particles have been successfully synthesised via the super-critical anti-solvent (SAS) and rapid expansion of super-critical solutions (RESS) processes, where the differences in the solubilities of solutes in super-critical fluids and several advantageous characteristics of super-critical fluids such as gas-like high diffusivities and low viscosities and liquid-like high mass densities are utilised for rapid syntheses of nano/micro particles.[25,26] Focusing on *critical opalescence*, it is supposed that incident light definitely hits fluids' molecules in fluids' systems set at or near the critical points and that ultraviolet (UV) photons may induce decomposition of fluids' molecules captured in large clusters without raising the molecular temperature. It has actually been demonstrated that carbon dioxide molecules are decomposed and carbon nano/micro particles are formed by irradiating a UV laser into carbon dioxide under its near-critical conditions at 31.0 °C, although UV photons are not absorbed by carbon dioxide.[27] It is therefore supposed that the dissociation of fluids' molecules and formation of carbon nanostructures in fluids under their near-critical conditions subjected to irradiation of UV photons may be universal phenomena.[27-30]

Here, we irradiate near-critical benzene set at 290 °C, in which either an alloy rod composed of mainly iron, chromium, and nickel is placed or copper complex molecules; bis(t-butylacetoacetato)copper(II): $Cu(tbaoac)_2$, are dissolved, with the second, third and fourth harmonics, the wavelength of which are, respectively, 532, 355 and 266 nm, generated from a neodymium doped yttrium/aluminium/garnet (Nd:YAG) laser. We show that benzene molecules are dissociated and various carbon structures such as fibres, coils, and metal-filling carbon nanoparticles are created. Particles

produced by laser ablation of the alloy rod act as a catalyst for the formation of fibres and metal-filling carbon nanoparticles, whereas those created via pyrolysis and photolysis of Cu(tbaoac)$_2$ act as a catalyst for the formation of carbon coils. The effect of the wavelength of the incident laser beam on the production of the above carbon nanostructures is investigated and clarified. The operational temperature of the present method is 290 °C, which is much lower than that of the conventional methods; e.g., laser ablation and CVD. Furthermore, the laser power density can be as low as 3.9 mW mm^{-2}. The experimental details are explained in the second section and the experimental results are shown and discussed in the third section. We summarise the results obtained in the present study in the final section.

Experimental details

First, we irradiated liquid benzene (99.5 %, Wako Pure Chemical Industries, Ltd.) confined in a glass container through a quartz window mounted at the top of the container with the second (532 nm), third (355 nm) and fourth (266 nm) harmonics generated from an Nd:YAG laser (Brilliant Quantel Co. Ltd.) at 25 °C and 1 atm to check any changes in colour and absorption spectra of liquid benzene. We measured the absorption spectra of liquid benzene at 25 °C and 1 atm before and after laser irradiation by ultraviolet-visible spectroscopy (DH2000-DUV, USB2000, Ocean Optics Inc.). We then carried out experiments of laser irradiation into benzene under near-critical conditions at 290 °C. The schematic diagram of the experimental system is shown in Fig. 1. Benzene was confined in a cylindrical stainless steel container. The inner and outer diameters, and inner and outer heights of the container were, respectively, 13 and 60 mm, and 19 and 66 mm. Two pieces of synthetic quartz were mounted at the top of the container for the introduction of a laser beam. The diameter and thickness of the upper synthetic quartz were 20 and 5 mm, whereas those of the lower quartz 20 and 10 mm. The mass density of benzene was set at 428 kg m^{-3}. A platinum resistance thermometer (Pt100, Chino Co. Ltd.) was embedded in the container wall. The temperature of benzene was regulated by a heater installed around the container and a PID controller (LT470, Chino Co. Ltd.). The accuracy of the temperature control was within ± 0.1 °C. The fluid conditions were changed from a sub-critical liquid-gas two-phase region at 25 °C to a near-critical one at 290 °C by controlling the fluid temperature. Note that the critical temperature, T_c, critical pressure, P_c, and critical mass density, ρ_c, of benzene are, respectively, 289 °C, 4.92 MPa, and 300 kg m^{-3}.[36] The mass density of benzene being constant, the pressure is thermodynamically determined once the temperature is set at a certain value. It is known that the state of sub-critical benzene is described by the Antoine equation,[37-41] whereas the state of super-critical benzene can be well described by the van der Waals equation.[41,42] Note that controlling the temperature is much easier and more precise than regulating the pressure. We irradiated a laser beam of 532, 355, or 266 nm wavelength into benzene under its near-critical conditions at 290 °C as mentioned. The diameter of the laser beam was 10 mm and the power density was set at 3.9 mW mm^{-2}. The duration of each laser pulse and the frequency of the pulse generation were 4.3 ns and 10 Hz. 50000 pulses of a laser beam were irradiated into benzene, in which either a cylindrical alloy rod composed of mainly iron, chromium and nickel (ISO-TR15510L No.26) was placed as a catalyst or copper complex

molecules; that is, bis(t-butylacetoacetato)copper(II)): Cu(tbaoac)$_2$, (99 %, Strem Chemical Inc.) were dissolved. The diameter and height of the catalytic alloy rod were 10 mm. The mass concentration of Cu(tbaoac)$_2$ was set at 3.47 mg ml^{-1}. After each experiment, the temperature was decreased gradually down to room temperature.

We observed the structures of the materials produced in the container by scanning electron microscopes (SEMs) (JSM-7400F, JEOL; SU8030, Hitachi Ltd.) and transmission electron microscopes (TEMs) (JEM2200FS, JEOL; JEM2100, JEOL). The elementary components of the structures were analysed by energy-dispersive X-ray spectroscopy (EDX) (JED2300T, JEOL). The size of the fibres and particles was measured targeting at least 100 samples from SEM images.

Results and discussion

First, we irradiated liquid benzene with laser at 25 °C and 1 atm to check any changes in colour and absorption spectra of liquid benzene as mentioned. The colour of liquid benzene changed significantly from transparent to yellow after irradiation of photons of 266 nm wavelength into liquid benzene, whereas there was no noticeable change in colour after irradiation of photons of 532 nm (see Fig. 2). In the case of the irradiation of photons of 355 nm wavelength, the colour of the liquid slightly changed (Fig. 2). The absorption spectra of liquid benzene at 25 °C and 1 atm after the laser irradiation is shown in Fig. 2, where the raw absorption spectra after the irradiation are subtracted by those before the laser irradiation. It is supposed that aromatic hydrocarbons such as naphthalene, biphenyl, and anthracene, and amorphous carbon were produced by photo-dissociation of benzene induced by a laser of 266 nm wavelength, noting that it is well known that photons of 240 - 280 nm wavelengths are absorbed by liquid benzene,[32,33] whereas the absorption spectrum hardly changed after irradiation of photons of 532 nm wavelength into benzene.

We then irradiated Nd:YAG laser into benzene, in which an alloy rod was placed, under its near-critical conditions at 290 °C. We observed the structures of materials produced in near-critical benzene by SEMs and TEMs and confirmed that amorphous and graphitic carbon structures, carbon fibres, and iron/chromium-filling carbon nanoparticles were created after irradiation of laser beams of 532, 355, and 266 nm wavelengths into near-critical benzene. Figure 3 shows SEM images of carbon fibres and iron/chromium-filling carbon nanoparticles created in near-critical benzene. Carbon fibres and iron/chromium-filling carbon nanoparticles were evenly formed on the surface of the catalytic alloy rod after irradiation of photons of 532 nm wavelength into near-critical benzene, while carbon fibres were not uniformly distributed on the surface of the alloy rod and the quantity of iron/chromium-filling carbon nanoparticles was very small in the case of irradiation of photons of 355 and 266 nm (see also Fig. S1 in the Supporting Information for SEM images of low magnifications of the fibres). According to the TEM image and EDX mappings shown in Fig. 4(a)-(c), a nickel particle was captured at the tip of each carbon fibre, which indicates that the particle acted as a catalyst. We also observed that nanoparticles composed of iron and chromium were encapsulated in carbon shells (Fig. 4(d)-(g)). The structures of the carbon shells were mostly amorphous (see Fig. S2 in the Supplementary Information for TEM images of iron/chromium carbon nanoparticles). The diameter of

iron/chromium-filling carbon nanoparticles produced by irradiation of photons of 532 nm varied from 10 to 150 nm. The diameter of carbon fibres was changed depending on the wavelength of the incident laser beam (see Fig. S3 in the Supplementary Information for the diameter distributions of carbon fibres). The diameter of carbon fibres created by irradiation of photons of 532, 355, and 266 nm wavelengths, respectively, ranged from 70 nm to 3.5 µm, 70 to 850 nm, and 20 to 400 nm. Note that the diameter distribution of fibres created by irradiation of photons of 532 nm wavelength was particularly broad since a number of catalytic nanoparticles were produced by irradiation of photons of 532 nm and those nanoparticles coagulated to form larger particles during the formation and growth process of the fibres. The maximum length of carbon fibres was approximately 0.1 mm irrespective of the wavelength of the incident laser. The diameter of the fibres decreased as the wavelength of incident photons decreased since the diameter of metal nanoparticles created by laser ablation, which acted as a catalyst, decreased with a decrease in the wavelength of photons.[34] The diameter of nanoparticles created by irradiation of photons of 532, 355, and 266 nm wavelengths in the air was, respectively, 180 ± 120, 140 ± 100, and 100 ± 70 nm (see Fig. S4 in the Supplementary Information for SEM images of nanoparticles created on the surface of the alloy rods by laser ablation).[34] Thin and short carbon fibres were created by irradiating photons of 266 nm wavelength, whereas thick and long ones were created by laser irradiation of 532 nm, noting that the maximum length of the fibres was more or less the same irrespective of the wavelength of incident laser beams as mentioned. It is worth stressing that benzene molecules were dissociated and carbon fibres and iron/chromium-filling carbon nanoparticles were efficiently created by irradiating photons of 532 nm wavelength into benzene under near-critical conditions at 290 °C, although liquid benzene was not dissociated at 25 °C and 1 atm after irradiation of photons of 532 nm as mentioned (see also Fig. 2). It is supposed as explained in Ref.33 that at least two- or three-photon absorption is required for the dissociation of a hydrogen atom from a benzene molecule since the photon energies of 532, 355, and 266 nm wavelengths are, respectively, 2.33, 3.50, and 4.66 eV, knowing that the dissociation energy is 4.90 eV.[35] The dissociation energy of a second hydrogen atom is lower than that of the first one once the first hydrogen atom has been dissociated, which is lower than the energy of a single photon of 355 and 266 nm. Therefore, six-membered rings of carbon atoms may be quite easily produced by irradiation of the third (355 nm) and fourth (266 nm) harmonics, whereas in the case of the second (532 nm) harmonic photons, two-photon absorption is still required to dissociate a second hydrogen atom from a benzene molecule.[40] We suppose that the possibility of multi-photon absorption increases as the state of benzene approaches its critical point due to the formation of large flexible molecular clusters.[27] The weight of carbon structures formed by laser irradiation increased with a decrease in the wavelength of incident photons (see Fig. S5 in the Supplementary Information for the weight of carbon structures created after irradiation of photons of 532, 355, and 266 nm wavelengths into benzene). In terms of the creation of carbon fibres and iron/chromium-filling carbon nanoparticles, however, irradiation of photons of a short wavelength; i.e., 266 nm, was not very efficient, in which case amorphous carbon was mostly created due to high absorption of photons by benzene and the less number of catalytic nanoparticles since photons of 266 nm

could not reach the alloy rod placed at the bottom of the container, whereas a number of metal nanoparticles were formed by ablation in the case of irradiation of photons of 532 nm, thanks to which carbon fibres and iron/chromium-filling carbon nanoparticles were efficiently formed in near-critical benzene at 290 °C. We suppose that liquid particles were initially produced by laser ablation of the alloy rod, considering the energy of a single photon of 532 nm wavelength is 2.33 eV. Liquid particles were finally transformed to solid ones during the cooling process of the particles. The phase transformation may be explained by the ternary phase diagram under high pressure, but in the present study, at least nickel and iron/chromium particles were formed; the former initiated the growth of carbon fibres, whereas the latter encouraged the formation of metal-filling carbon nanoparticles. Nevertheless, if catalytic nanoparticles are produced and placed on a substrate in advance, carbon fibres and iron/chromium-filling carbon nanoparticles were efficiently created even by irradiation of photons of 266 nm wavelength as in the case of irradiation of photons of 532 nm wavelength (see Fig. S6 in the Supplementary Information for the formation of carbon fibres created in benzene by irradiation of photons of 266 nm wavelength).

Carbon fibres were also created by irradiating a laser beam of 532, 355, and 266 nm wavelengths into benzene, in which $Cu(tbaoac)_2$ was dissolved, under near-critical conditions at 290 °C. Most of the carbon fibres were coiled (see Fig. 5). It is known that polygonal metal nanoparticles initiate the formation of coiled carbon fibres due to the difference in the diffusion speed of carbon atoms in the particles depending on the polygonal facet.[36] The diameter of the coils created by the second (532 nm), third (355 nm), and fourth (266 nm) harmonics was, respectively, 300 ± 80, 185 ± 90, and 170 ± 55 nm, while the helical diameter was 970 ± 610, 550 ± 420, and 365 ± 190 nm. According to the EDX mappings of the coils, which are shown in Fig. 5(d)-(f), a copper particle was encapsulated at the tip of each coil. The size of a copper particle formed after irradiation of a laser beam of 532, 355, and 266 nm wavelengths was 220 ± 50, 110 ± 100, and 100 ± 60 nm. Thermogravimetric analysis (TGA) of $Cu(tbaoac)_2$ carried out in nitrogen at a flow rate of 100 ml min^{-1} showed that the melting and pyrolytic decomposition temperatures of $Cu(tbaoac)_2$ were, respectively, 110 and 190 °C[43] and we confirmed that copper particles and films were formed on the inner surface of the quartz window and the container at 290 °C (see Figs. S7 and S8 in the Supplementary Information for the TGA of $Cu(tbaoac)_2$ and an SEM image of nanoparticles created by pyrolytic decomposition of $Cu(tbaoac)_2$).[43] We therefore suppose that polygonal copper nanoparticles were formed by both pyrolytic and photo decomposition of $Cu(tbaoac)_2$ in benzene and the growth of carbon coils was initiated on the catalytic polygonal copper nanoparticles, which had been deposited on the inner surface of the quartz window. Carbon coils were efficiently created by irradiation of photons of 355 and 266 nm wavelengths thanks to the effective dissociation of benzene near the quartz window and catalytic nanoparticles deposited on the surface of quartz window. Note that photons of short wavelengths cannot penetrate benzene under near-critical conditions as mentioned, but can dissociate benzene molecules near the quartz window. The diameter of the fibres decreased with a decrease in the wavelength of a laser beam since the size of the catalytic particles decreased as the wavelength of photons decreases.[34]

In this study, we developed a low temperature synthetic methodology utilising near-critical benzene. Carbon nanostructures such as fibres and metal-filling carbon nanoparticles were formed under near-critical conditions. The laser power density was as low as 3.9 mW mm^{-2} and the effect of the wavelength of incident laser beams on the creation of carbon nanostructures was clarified. Note that carbon fibres were previously synthesised by the hyperbaric-pressure laser chemical vapour deposition method using benzene, but the pressure was set at up to only 0.25 MPa.[44] Carbon nanoparticles were produced by decomposing liquid benzene by a femto-second laser beam, but the laser power density was as high as 1 TW mm^{-2}.[45] We demonstrated that there are two ways of producing carbon fibres; that is, irradiation of a laser beam into near-critical benzene, in which either (a) a solid alloy rod is placed or (b) complex molecules are dissolved. In the former case, the surface of the rod was ablated by laser and nanoparticles, which acted as a catalyst, were formed, whereas in the latter case, Cu(tbaoac)$_2$ was decomposed via both pyrolysis and photolysis and catalytic nanoparticles were formed. In the former case, irradiation of photons of 532 nm wavelength into benzene under near-critical conditions at 290 °C worked efficiently for the formation of carbon fibres and metal-filling carbon nanoparticles, although the energy of a single photon of 532 nm is lower than that of 355 and 266 nm and photons of 532 nm are not absorbed by benzene under standard conditions, whereas in the latter case, fibres were efficiently produced by irradiation of photons of 355 and 266 nm since the catalytic nanoparticles were deposited on the inner surface of a quartz window and the dissociation of benzene was encouraged by photons of those short wavelengths near the window. Interestingly, when a laser beam of 266 nm wavelength was irradiated into near-critical benzene, in which metallocenes were dissolved, neither fibres nor coils were formed, but only metal-filling carbon nanoparticles were created,[30] whereas in the present case, fibres and coils were successfully produced. We suppose that aligned carbon fibres can be grown by irradiating photons of 532 nm wavelength into near-critical benzene, in which pre-arranged catalytic nanoparticles are placed on a substrate, or by irradiating photons of 335 or 266 nm into benzene through a quartz window, on the inner surface of which pre-arranged catalytic nanoparticles are deposited.

Conclusions

We irradiated the second (532 nm wavelength), third (355 nm), and fourth (266 nm) harmonics generated from an Nd:YAG laser into near-critical benzene, in which either an alloy rod was placed or Cu(tbaoac)$_2$ was dissolved, at 290 °C and found that carbon fibres and coils, and metal-filling carbon nanoparticles were created via the interactions among the incident photons, catalytic nanoparticles and benzene molecules captured in large clusters formed under near-critical conditions. The size of carbon fibres and coils was dependant on the wavelength of the incident photons. Carbon fibres and coils, and metal-filling carbon nanoparticles were efficiently created by irradiating photons of 532 nm wavelength into benzene, in which an alloy rod was placed, under near-critical conditions, although photons of 532 nm are not absorbed by liquid benzene under standard conditions and the energy of a single photon of 532 nm is lower than that of 355 and 266 nm. When Cu(tbaoac)$_2$ was dissolved in benzene under near-critical

conditions, irradiation of 355 and 266 nm wavelengths efficiently created carbon coils. The operational temperature of the present synthetic method is much lower than that of the conventional synthetic methods of nano materials and what is more, the laser power density can be as low as 3.9 mW mm^{-2}.

Acknowledgements

References

1 F.P. Bundy, H.T. Hall, H.M. Strong and R.H. Wentorf, *Nature*, 1955, **176**, 51-55.

2 S. Motojima, M. Kawaguchi, K. Nozaki and H. Iwanaga, *Appl. Phys. Lett.*, 1990, **56**, 321-323.

3 H.W. Kroto, J.R. Heath, S.C. O'Brien, R.F. Curl and R.E. Smalley, *Nature*, 1985, **318**, 162-163.

4 S. Iijima, *Nature*, 1991, **354**, 56-58.

5 A.K. Geim and K.S. Novoselov, *Nat. Mater.*, 2007, **6**, 183-191.

6 S. Motojima, X. Chen, S. Yang and M. Hasegawa, *Diam. Relat. Mater.*, 2004, **13**, 1989-1992.

7 R. Hao, R.J. Xing, Z.C. Xu, Y.L. Hou, S. Gao and S.H. Sun, *Adv. Mater.*, 2010, **22**, 2729-2742.

8 B. Sivakumar, R.G. Aswathy, R. Sreejith Y. Nagaoka, S. Iwai, M. Suzuki, T. Fukuda, T. Hasumura, Y. Yoshida, T. Maekawa and D. Sakthikumar, *J. Biomed. Nanotechnol.*, 2014, **10**, 885-899.

9 A. Kumar, P.K. Jena, S. Behera, R.F. Lockey, S. Mohapatra and S. Mohapatra, *Nanomed. Nanotechnol.*, 2010, **6**, 64-69.

10 T. Guo, P. Nikolaev, A. Thess, D.T. Colbert and R.E. Smalley, *Chem. Phys. Lett.*, 1995, **243**, 49-54.

11 A. Thess, R. Lee, P. Nikolaev, H. Dai, P. Petit, J. Robert, C. Xu, Y.H. Lee, S.G. Kim, A.G. Rinzler, D.T. Colbert, G.E. Scuseria, D. Tománek, J.E. Fischer and R.E. Smalley, *Science*, 1996, **273**, 483-487.

12 M. José-Yacamán, M. Miki-Yoshida, L. Rendón and J.G. Santiesteban, *Appl. Phys. Lett.*, 1993, **62**, 657-659.

13 H.E. Stanley, *Introduction to Phase Transition and Critical Phenomena*, Oxford University Press, Oxford, 1971.

14 S.-K. Ma, *Modern theory of Critical Phenomena*, ed. S.-K. Ma., Westview press, New York, 2000.

15 L.P. Kadanoff, *Statistical Physics: Statics, Dynamics and Renormalization*, ed. L.P. Kadanoff, World Scientific, New Jersey, 2000.

16 A. Onuki, H. Hao and R.A. Ferrell, *Phys. Rev. A.*, 1990, **41**, 2256-2259.

17 K. Ishii, T. Maekawa, H. Azuma, S. Yoshihara and M. Onishi, *Appl. Phys. Lett.*, 1998, **72**, 16-18.

18 T. Maekawa, K. Ishii, Y. Shiroishi and H. Azuma, *J. Phys. A: Math. Gen.*, 2004, **37**, 7955-7969.

19 H. Hu, T. He, J. Feng, M. Chen and R. Cheng, *Polymer*, 2002, **43**, 6357-6361.

20 E. Lester, P. Blood, J. Denyer, D. Giddings, B. Azzopardi and M.

COMMUNICATION

Poliakoff, *J. Supercrit. Fluids*, 2006, **37**, 209-214.

21 K. Jinno, H. Nagashima, K. Itoh, M. Saito and M. Buonoshita, *Fresenius J. Anal. Chem.*, 1992, **344**, 435-441.

22 R.N. Patel, S. Bandyopadhyay and A. Ganesh, *Bioresource Technol.*, 2006, **97**, 847-853.

23 E. Bok, D. Kelch and K.S. Schmachuer, *Solid State Technol.*, 1992, **35**, 117-120.

24 E.M. Vaquero, S. Beltrán and M.T. Sanz, *J. Supercrit. Fluids*, 2006, **37**, 142-150.

25 O. Boutin, E. Badens, E. Carretier and G. Charbit, *J. Supercrit. Fluids*, 2004, **31**, 89-99.

26 P.S. Shah, T. Hanrath, K.P. Johnston and B.A. Korgel, *J. Phys. Chem. B*, 2004, **108**, 9574-9587.

27 T. Fukuda, T. Maekawa, T. Hasumura, N. Rantonen, K. Ishii, Y. Nakajima, T. Hanajiri, Y. Yoshida, R. Whitby and S. Mikhalovsky, *New J. Phys.*, 2007, **9**, 321-331.

28 T. Fukuda, N. Watabe, R. Whitby and T. Maekawa, *Nanotechnology*, 2007, **18**, 415604-415609.

29 T. Hasumura, T. Fukuda, R.L.D. Whitby, O. Aschenbrenner and T. Maekawa, *J. Nanopart. Res.*, 2011, **13**, 53-58.

30 Y. Hayasaki, T. Fukuda, T. Hasumura and T. Maekawa, *Adv. Nat. Sci.: Nanosci. Nanotechnol.*, 2012, **3**, 035010.

31 K.A. Kobe and R.E. Lynn Jr., *Chem. Rev.*, 1953, **52**, 117-236.

32 M. Hackett, H. Wang, G.C. Miller and D.J. Bornhop, *J. Chromatogr. A*, 1995, **695**, 243-257.

33 R. M. Silverstein, F. X. Webster and D. J. Kiemle, *Spectrometric Identification of Organic Compounds*, New York: Wiley, 2005.

34 T. Tsuji, K. Iryo, N. Watanabe and M. Tsuji, *Appl. Surf. Sci.*, 2002, **202**, 80–85.

35 S.J. Blanksby and G.B Ellison, *Acc. Chem. Res.*, 2003, **36**, 255-263.

36 X. Chen, S. Yang and S. Motojima, *Mater. Lett.*, 2002, **57**, 48-54.

37 C.B. Willingham, W.J. Taylor, J.M. Pignocco and F.D. Rossini, *J. Res. Natl. Bur. Stand.*, 1945, **35**, 219-244.

38 D.D. Kalafati, D.S. Rasskazov and E.K. Petrov, *Zh. Fiz. Khim.*, 1967, **41**, 1357-1359.

39 D.D. Deshpande and M.V. Pandya, *Trans. Faraday Soc.*, 1967, **63**, 2149-2157.

40 C. Eon, C. Pommier and G. Guiochon, *J. Chem. Eng. Data*, 1971, **16**, 408-410.

41 *CRC Handbook of Chemistry and Physics*, *Internet Version 2005*, ed. D.R. Lide, CRC Press, Boca Raton, FL, 2005.

42 J.O. Valderrama, *Ind. Eng. Chem. Res.*, 2003, **42**, 1603-1618.

43 A. Devi, J. Goswami, R. Lakshme and S.A. Shivashankar, *J. Mat. Res.*, 1998, **13**, 687-692.

44 J.L. Maxwell, M. Boman, R.W. Springer, J. Narayan and S. Gnanavelu, *J. Am. Chem. Soc.*, 2006, **128**, 4405-4413.

45 M.J. Wesolowski, S. Kuzmin, B. Moores, B. Wales, R. Karimi, A.A. Zaidi, Z. Leonenko, J.H. Sanderson and W.W. Duley, *Carbon*, 2011, **49**, 625-630.

ᶜ School of Pharmacy and Biomolecular Sciences, University of Brighton, Brighton BN2 4GJ, United Kingdom.

ᵈ School of Engineering, Nazarbayev University, Astana 010000, Republic of Kazakhstan.

† Electronic Supplementary Information (ESI) available: See DOI: 10.1039/c000000x/
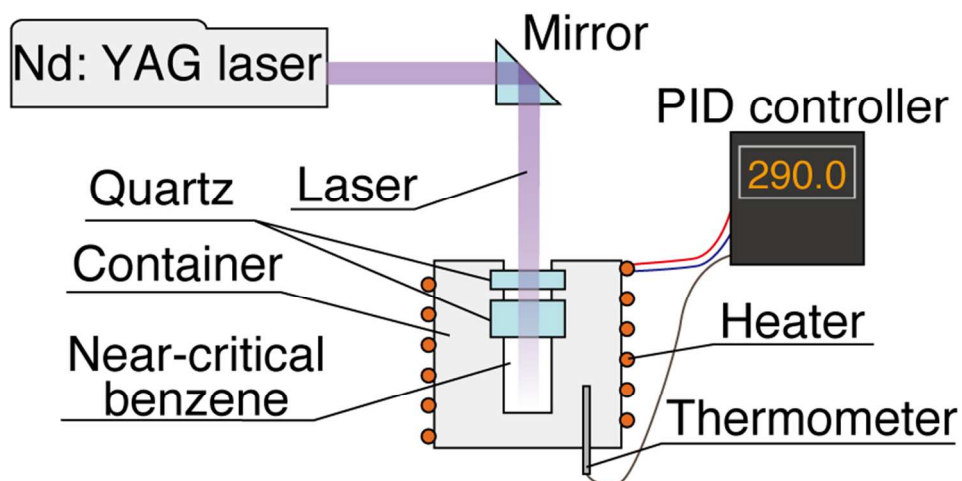
Figure captions

Fig. 1 Schematic diagram of the experimental system. Benzene is confined in a cylindrical stainless steel container. Two pieces of synthetic quartz are mounted at the top of the container for the introduction of a laser beam. The temperature is controlled by a heater installed around the container and a PID controller. The second (532 nm), third (355 nm) and fourth (266 nm) harmonics are irradiated into benzene under its near-critical conditions at 290 °C. Either a cylindrical alloy rod composed of mainly iron, chromium and nickel is placed on the surface of the bottom wall of the container as a catalyst or bis(t-butylacetoacetato)copper(II)); Cu(tbaoac)$_2$, is dissolved in benzene.

Fig. 2 Absorption spectra and photographs of benzene after irradiation of the second (532 nm), third (355 nm) and fourth (266 nm) harmonics into liquid benzene at 25 °C and 1 atm. The raw absorption spectra of benzene after irradiation of the laser were subtracted by those before irradiation. It is supposed that benzene was dissociated and some hydrocarbons of low molecular weights and amorphous carbon were created by irradiation of photons of 266 nm wavelength, whereas there was no significant change in the absorption spectra after irradiation of photons of 532 nm.

Fig. 3 SEM images of carbon structures created on the surface of a catalytic alloy rod in near-critical benzene after irradiation of a laser beam of different wavelengths. (a) Carbon fibres created by irradiation of photons of 532 nm wavelength. (b) Metal-filling carbon nanoparticles created by irradiation of photons of 532 nm. (c) Carbon fibres created by irradiation of photons of 355 nm. (d) Carbon fibres created by irradiation of photons of 266 nm.

Fig. 4 TEM images and EDX mappings of carbon fibres and metal-filling carbon nanoparticles created in near-critical benzene by irradiation of photons of 532 nm wavelength. (a) TEM image of carbon fibres. (b) EDX mapping of carbon corresponding to TEM image (a). (c) EDX mapping of nickel corresponding to TEM image (a). (d) TEM image of iron/chromium-filling carbon nanoparticles. (e) EDX mapping of carbon corresponding to TEM image (d). (f) EDX mapping of iron corresponding to TEM image (d). (g) EDX mapping of chromium corresponding to TEM image (d).

Fig. 5 SEM and TEM images of carbon fibres created after irradiation of a laser beam of 532, 355 and 266 nm wavelengths into near-critical benzene. Cu(tbaoac)$_2$ was dissolved in benzene. (a) SEM image of carbon fibres created by irradiation of photons of 532 nm wavelength. (b) SEM image of carbon fibres created by irradiation of photons of 355 nm. (c) SEM image of carbon fibres created by irradiation of photons of 266 nm. (d) TEM image of carbon fibres created by irradiation of 355 nm. (e) EDX mapping of carbon corresponding to TEM image (d). (f) EDX mapping of copper corresponding to TEM image (d).

ᵃ Bio-Nano Electronics Research Centre, Toyo University, Kawagoe 350-8585, Japan. E-mail: maekawa@toyo.jp, Tel: +81 492391375

ᵇ Graduate School of Interdisciplinary New Science, Toyo University, Kawagoe 350-8585, Japan.

Schematic diagram of the experimental system. Benzene is confined in a cylindrical stainless steel container. Two pieces of synthetic quartz are mounted at the top of the container for the introduction of a laser beam. The temperature is controlled by a heater installed around the container and a PID controller. The second (532 nm), third (355 nm) and fourth (266 nm) harmonics are irradiated into benzene under its near-critical conditions at 290 °C. Either a cylindrical alloy rod composed of mainly iron, chromium and nickel is placed on the surface of the bottom wall of the container as a catalyst or bis(t-butylacetoacetato)copper(II)); Cu(tbaoac)2, is dissolved in benzene.
80x39mm (300 x 300 DPI)
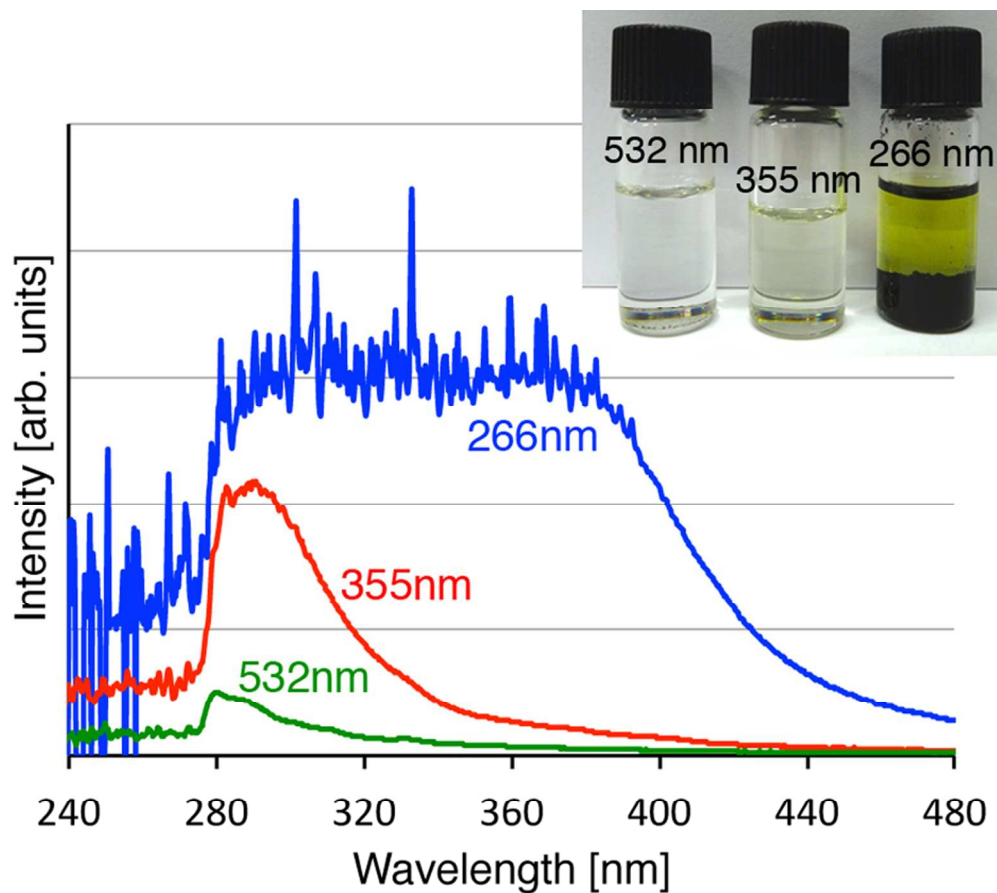
Absorption spectra and photographs of benzene after irradiation of the second (532 nm), third (355 nm) and fourth (266 nm) harmonics into liquid benzene at 25 °C and 1 atm. The raw absorption spectra of benzene after irradiation of the laser were subtracted by those before irradiation. It is supposed that benzene was dissociated and some hydrocarbons of low molecular weights and amorphous carbon were created by irradiation of photons of 266 nm wavelength, whereas there was no significant change in the absorption spectra after irradiation of photons of 532 nm.
80x71mm (300 x 300 DPI)
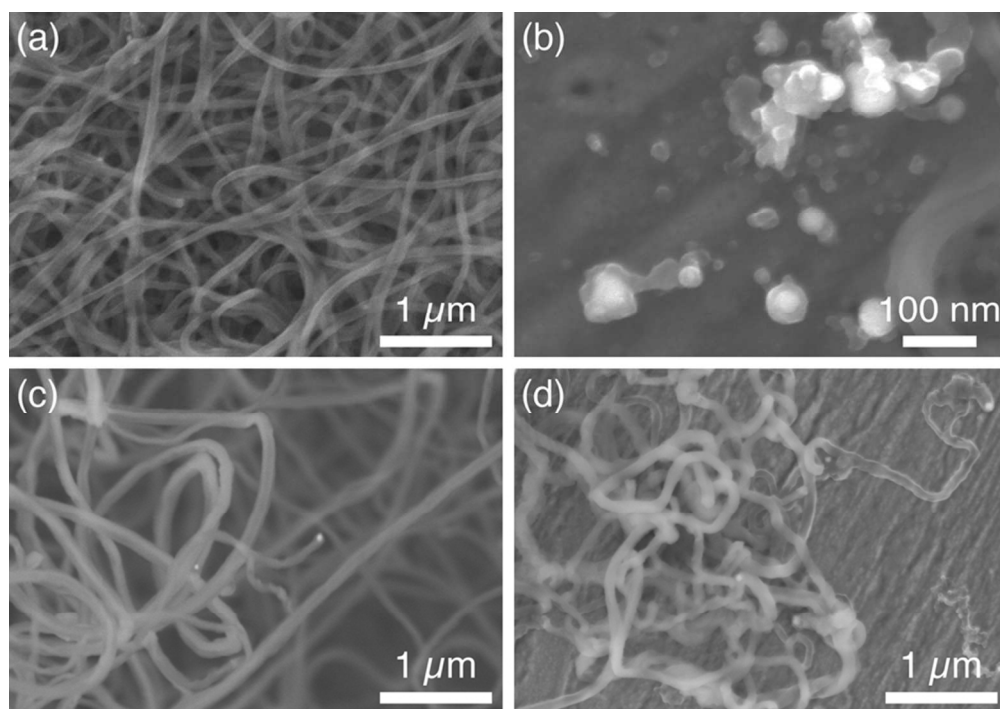
SEM images of carbon structures created on the surface of a catalytic alloy rod in near-critical benzene after irradiation of a laser beam of different wavelengths. (a) Carbon fibres created by irradiation of photons of 532 nm wavelength. (b) Metal-filling carbon nanoparticles created by irradiation of photons of 532 nm. (c) Carbon fibres created by irradiation of photons of 355 nm. (d) Carbon fibres created by irradiation of photons of 266 nm.
80x56mm (300 x 300 DPI)
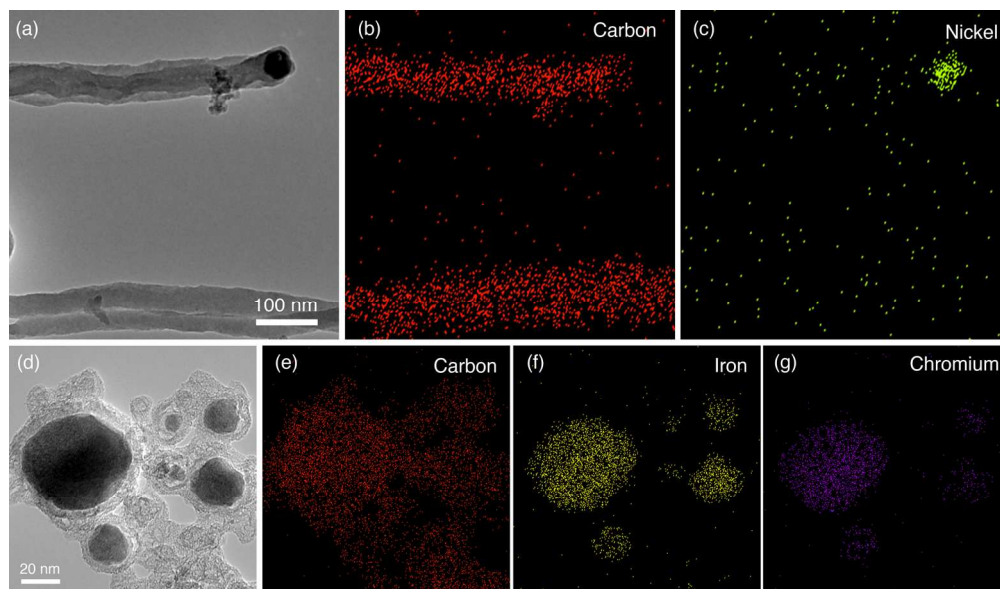
TEM images and EDX mappings of carbon fibres and metal-filling carbon nanoparticles created in near-critical benzene by irradiation of photons of 532 nm wavelength. (a) TEM image of carbon fibres. (b) EDX mapping of carbon corresponding to TEM image (a). (c) EDX mapping of nickel corresponding to TEM image (a). (d) TEM image of iron/chromium-filling carbon nanoparticles. (e) EDX mapping of carbon corresponding to TEM image (d). (f) EDX mapping of iron corresponding to TEM image (d). (g) EDX mapping of chromium corresponding to TEM image (d).
166x97mm (300 x 300 DPI)
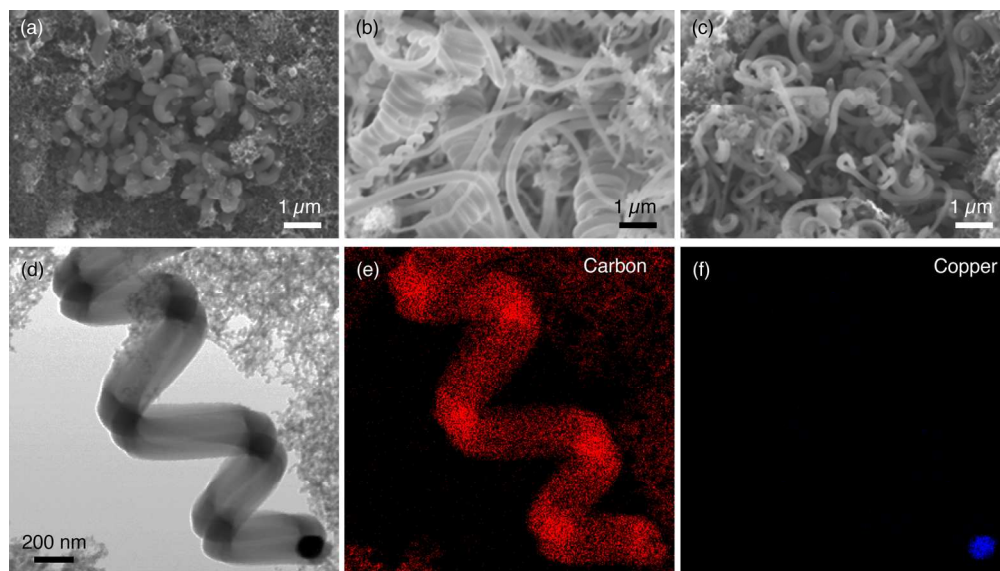
SEM and TEM images of carbon fibres created after irradiation of a laser beam of 532, 355 and 266 nm wavelengths into near-critical benzene. Cu(tbaoac)2 was dissolved in benzene. (a) SEM image of carbon fibres created by irradiation of photons of 532 nm wavelength. (b) SEM image of carbon fibres created by irradiation of photons of 355 nm. (c) SEM image of carbon fibres created by irradiation of photons of 266 nm. (d) TEM image of carbon fibres created by irradiation of 355 nm. (e) EDX mapping of carbon corresponding to TEM image (d). (f) EDX mapping of copper corresponding to TEM image (d). 166x94mm (300 x 300 DPI)